



Published in final edited form as:

J Immunol. 2010 September 15; 185(6): 3227–3238. doi:10.4049/jimmunol.0903066.

Crosstalk Between PKA and Epac Regulates the Phenotypic Maturation and Function of Human Dendritic Cells¹

Jone Garay^{*}, June A. D'Angelo^{*}, YongKeun Park[†], Christopher M. Summa[‡], Martha L. Aiken[§], Eric Morales[§], Kamran Badizadegan[¶], Edda Fiebiger^{||}, and Bonny L. Dickinson^{*,§}

^{*} Department of Microbiology, Immunology, and Parasitology, Louisiana State University Health Science Center, New Orleans, LA 70112

[†] George R. Harrison Spectroscopy Laboratory, Massachusetts Institute of Technology, Cambridge, MA 02139

[‡] The Research Institute for Children, Children's Hospital and Department of Computer Science, University of New Orleans, LA 70148

[§] The Research Institute for Children, Children's Hospital and Department of Pediatrics, Louisiana State University Health Science Center, New Orleans, LA 70118

[¶] Department of Pathology, Harvard Medical School and Massachusetts General Hospital, Boston, MA 02115

^{||} Division of Gastroenterology and Nutrition, Children's Hospital Boston, Harvard Medical School, Boston, MA 02115

Abstract

The cAMP-dependent signaling pathways that orchestrate dendritic cell (DC) maturation remain to be defined in detail. While cAMP was previously thought to signal exclusively through PKA, it is now clear that cAMP also activates Epac, a second major cAMP effector. Whether cAMP signaling via PKA is sufficient to drive DC maturation or whether Epac plays a role has not been examined. Here, we used cAMP analogs to selectively activate PKA or Epac in human monocyte-derived DCs and examined the effect of these signaling pathways on several hallmarks of DC maturation. We show that PKA activation induces DC maturation as evident by the increased cell surface expression of MHC class II, co-stimulatory molecules and the maturation marker CD83. PKA activation also reduces DC endocytosis and stimulates chemotaxis to the lymph node-associated chemokines CXCL12 and CCL21. Although PKA signaling largely suppresses cytokine production, the net effect of PKA activation translates to enhanced DC activation of allogeneic T cells. In contrast to the stimulatory effects of PKA, Epac signaling has no effect on DC maturation or function. Rather, Epac suppresses the effects of PKA when both pathways are activated simultaneously. These data reveal a previously unrecognized crosstalk between the PKA and Epac signaling pathways in DCs and raise the possibility that therapeutics targeting PKA may generate immunogenic DCs while those that activate Epac may produce tolerogenic DCs capable of attenuating allergic or autoimmune disease.

¹This work was supported by a grant from the Louisiana Board of Regents NSF(2008)-PFUND-101 awarded to B.L.D., a LSUHSC Research Enhancement Fund New Project Grant awarded to B.L.D., NIH grant P41-RR02594 awarded to the Massachusetts Institute of Technology Laser Biomedical Research Center, NIH grant R01AI075037 awarded to E.F., and funds from the Research Institute for Children.

Corresponding author information: Bonny L. Dickinson, PhD, The West Virginia School of Osteopathic Medicine, 400 North Lee Street, Lewisburg, WV 24901. Tel: (304) 647-6370; bdickinson@oste.wvso.edu.

Disclosures

The authors have no financial conflict of interest.

Introduction

Tissue resident dendritic cells (DCs) scan the periphery for antigen (1). Following exposure to antigens containing “danger signals” such as toll-like receptor (TLR) ligands, DCs undergo functional maturation. Maturation involves up-regulation of chemokine receptors that promote migration to lymph nodes, down-regulation of antigen capture by endocytosis, changes in cytokine production and an increase in the surface expression of MHC class II and co-stimulatory molecules required for antigen presentation and T cell activation (2,3). The transition of an immature DC to the mature form is critical as only mature DCs can activate T cells to initiate adaptive immunity. Indeed, DCs that are arrested in an immature or semi-mature state induce T cell anergy resulting in the development of tolerance (4–6). Elucidating the molecular mechanisms that drive DC maturation is relevant for the design of DC-based cancer vaccines, particularly now as the first DC-based vaccine has been approved in the U.S. to treat patients with advanced prostate cancer (7). Despite recent advances, there is a clear need to improve the efficacy of DC-based immunotherapeutics (8–12). Current efforts are focused on the development of novel stimuli for *ex vivo* conditioning of therapeutic DCs to promote their maturation and migration to lymph nodes for T cell priming.

In addition to TLR ligands, cAMP-elevating molecules also induce DC maturation and yet the role of cAMP signaling in the context of DC immunotherapy has not been studied. A variety of endogenous molecules stimulate DC maturation via the activation of cAMP signaling, including lipid mediators (prostaglandin E2), hormones (norepinephrine), neuropeptides (vasoactive intestinal peptide), complement components (C3a) and nucleotides (adenosine and ATP) as well as bacterial toxins such as the mucosal adjuvant cholera toxin (CT) and the anthrax edema toxin (13–19). However, the underlying molecular mechanisms by which cAMP regulates DC maturation remain to be fully elucidated. While cAMP was previously thought to signal exclusively through PKA, it is now clear that cAMP also activates Epac, the guanine nucleotide exchange factor for the small GTPase Rap1 (20). Epac controls several functions once ascribed to PKA and studies show that PKA and Epac may act independently, converge synergistically or function antagonistically to regulate specific cellular functions (20–22). A major gap in our understanding of cAMP signaling as it relates to DC maturation is whether Epac plays a role, and if so, whether crosstalk between the PKA and Epac signaling pathways controls this process.

Here, we addressed the hypothesis that cAMP activation of Epac plays a role in regulating the maturation and function of human monocyte-derived DCs. Because cAMP binds to both PKA and Epac with the same affinity (23), differentiating between the roles of PKA and Epac in cAMP-dependent cellular processes has been difficult. The recent synthesis and characterization of cAMP analogs that selectively bind and activate either PKA or Epac have now made it possible to discriminate between the two signaling pathways (24). We used highly selective cAMP analogs to examine the effect of PKA and Epac signaling on several hallmarks of DC maturation including the up-regulation of MHC class II and co-stimulatory molecules, chemotaxis to lymph node-associated chemokines, down-regulation of endocytosis, changes in cytokine expression and T cell activation. We also analyzed the effect of PKA and Epac signaling on two forms of non-directed DC migration: migration in the absence of chemical cues (random migration) and migration in symmetrical concentrations of chemoattractants (chemokinesis). Our data reveal a previously unrecognized crosstalk between the PKA and Epac signaling pathways in DCs. The results of this study suggest that elucidating the points of interaction between the PKA and Epac signaling pathways will be critical for understanding how cAMP signaling is integrated in DCs to affect the initiation or inhibition of T cell-mediated immune responses *in vivo*.

Materials and Methods

Reagents and antibodies

Cholera toxin (CT) was obtained from Calbiochem (San Diego, CA, USA). *Escherichia coli* 026:B6 lipopolysaccharide (LPS; γ -irradiated; total impurities <5% protein) and FITC-dextran (40,000 Da) were from Sigma (St. Louis, MI, USA). IBMX (3-isobutyl-1-methylxanthine) was obtained from Alexis Biochemicals (Farmingdale, NY, USA). N⁶-benzoyladeniosine-3', 5'-cyclic monophosphate (6-Bnz-cAMP; an inefficient Epac activator and a full PKA activator) (25) was from Sigma and 8-(4-chlorophenylthio)-2'-O-methyl-cAMP (O-Me-cAMP; the combination of 8-pCPT- and 2'-O-methyl substitutions in this cAMP analog improved the Epac/PKA binding selectivity approximately three orders of magnitude) (25) was from Biolog Life Science Institute (Bremen, Germany). 6-Bnz-cAMP was dissolved in water and O-Me-cAMP was dissolved in DMSO. Dibutyryl cAMP (db-cAMP) was purchased from Sigma. Recombinant human CXCL12, recombinant human CCL21, mouse anti-human CXCR4 monoclonal antibody (clone 12G5), mouse anti-human CCR7 monoclonal antibody (clone 150503), mouse IgG isotype controls, and recombinant human IL-4 were purchased from R&D Systems (Minneapolis, MN, USA). Phosphatase inhibitors were from Sigma. Phospho-CREB (Ser 133) and CREB rabbit antibodies were from Cell Signaling Technology, Inc. (Danvers, MA, USA). The goat anti-rabbit IgG antibody conjugated to horseradish peroxidase was from Sigma and the goat anti-mouse IgG conjugated to FITC was from R&D Systems. Recombinant human GM-CSF (Leukine) was from Berlex Laboratories Inc. (Montville, NJ, USA). RPMI 1640, FBS, penicillin, streptomycin sulfate, and amphotericin B were from Invitrogen (Carlsbad, CA, USA). The following FITC-conjugated mouse monoclonal antibodies were purchased from BD Pharmingen (San Jose, CA, USA): IgG1k, IgG2a, anti-CD80, anti-CD83, anti-CD86, anti-CD3, anti-CD19, and anti-HLA-DR.

Human monocyte-derived dendritic cells

Human peripheral blood mononuclear cells (PBMCs) were isolated from normal human buffy coats (purchased from the Blood Donation Center of Louisiana) by centrifugation on Ficoll-Paque (GE Healthcare, Uppsala, Sweden). Monocytes were purified from PBMCs by positive selection using immunomagnetic cell separation (Human CD14 Microbeads, Miltenyi Biotec, Auburn, CA, USA). To derive DCs, monocytes (10^6 cells per ml) were cultured in complete medium (RPMI 1640 supplemented with 10% heat-inactivated FBS, 10U/ml penicillin, 10 μ g/ml streptomycin sulfate, and 25ng/ml amphotericin B) containing IL-4 (10ng/ml; 290 U/ml) and GM-CSF (100ng/ml; 560 U/ml) for 4–5 days in a humidified atmosphere at 37°C with 5% CO₂. Medium containing fresh cytokines was replenished every other day during culture. Immature DCs were treated with compounds on day 4 or 5 and cultured for 24 h before analysis. DC preparations routinely contained negligible quantities of CD3+ T cells ($0.54 \pm 0.51\%$) (Ave \pm SD) and CD19+ B cells ($1.44 \pm 1.71\%$) (Ave \pm SD). The average percentage of granulocytes (eosinophils and neutrophils) in DC preparations from three separate buffy coats was $10 \pm 4\%$ (Ave \pm SD) and the average percentage of DCs was $92 \pm 3\%$ (Ave \pm SD) as determined by Wright stain of CytoSpins (Diff-Quik, Baxter Scientific, Deerfield, IL, USA). The Institutional Review Boards of LSU Health Sciences Center and the Children's Hospital of New Orleans have approved these studies.

Human T cell isolation

CD3+ T cells were isolated from the CD14-negative cell population obtained following the purification of monocytes from normal human buffy coats (Pan T Cell Isolation Kit, Miltenyi Biotec).

Immunoblot detection of phospho-CREB and total CREB

DCs were lysed in RIPA buffer (50mM Tris, pH 7.4, 150mM NaCl, 1% Nonidet P-40, 0.5% sodium deoxycholate, 0.1% SDS) containing phosphatase inhibitors (10mM sodium pyrophosphate, 1mM Na₃VO₄ and 50mM NaF) and protease inhibitors (Complete Protease Inhibitor Cocktail Tablets; Roche, Nutley, NJ, USA). Lysates were briefly centrifuged to remove insoluble material and the protein content was determined using the Pierce BCA (bicinchoninic acid) Protein Assay kit (Thermo Scientific, Rockford, IL, USA). Then, equal quantities of protein were separated by reducing SDS-PAGE and transferred to nitrocellulose (Bio-Rad Laboratories, Hercules, CA, USA). The nitrocellulose was blocked in PBS containing 5% milk followed by incubated with rabbit phospho-CREB and total CREB antibodies. Rabbit antibodies were detected with a goat anti-rabbit IgG antibody conjugated to horseradish peroxidase. Signals were detected using the Pierce Thermo Scientific SuperSignal West Femto chemiluminescent substrate system. Band intensities were quantified by densitometry using a Bio-Rad VersaDoc Imaging System.

Endotoxin detection

The endotoxin level in CT was determined using the Limulus assay (E-toxate; Sigma) following manufacturer's instructions. We found that 0.5mg/ml of CT, a quantity 500-times greater than the amount used in our assays, contained ≤ 0.125 EU/ml of endotoxin.

Chemotaxis, random migration, and chemokinesis assays

To measure chemotaxis, DCs (10^5 cells in 0.1ml of serum-free RPMI containing 0.5% BSA and 10mM Hepes, pH 7.4) were added to the upper chambers of 0.33cm² Transwell filters (5.0 μ m-pore; Corning, Lowell, MA, USA) and CXCL12 or CCL21 in a 0.6ml volume in the same medium was added to the lower well. To measure random migration, 0.6ml of medium without chemokine was placed into the lower well and for chemokinesis studies CXCL12 was present in the medium of both the upper and lower chambers. DCs were incubated in Transwells for 90 min at 37°C under 5% CO₂. Following incubation, the filters were carefully removed and 0.5ml of the medium in the lower well was collected and added to tubes containing 0.5ml 4% paraformaldehyde in PBS. The number of migrated DCs was determined by counting cells for 1 min in a flow cytometer (LSR II, Becton Dickinson, Franklin Lakes, NJ, USA) at a constant flow rate (~30 μ l per min). In experiments in which we analyzed chemokinesis, the number of migrated DCs was determined by counting cells for 2 min. The chemotactic index represents the fold-change in the number of cells that migrated in response to the chemoattractant divided by the basal migration of cells that migrated in response to control medium. In the chemokinesis assays, the chemotactic index is the number of DCs that migrated in response to a gradient of CXCL12 divided by the number of DCs that migrated in symmetrical concentrations of CXCL12. Data are plotted as the mean \pm SEM of triplicate measurements from 2–4 independent experiments. Each experiment was performed with DCs derived from different donors.

Flow cytometry

Cells were resuspended at 10^5 cells per 0.1ml of flow buffer (PBS containing 0.5% BSA) and incubated with FITC-conjugated primary antibodies for 20 min at 4°C. Cells were then fixed with 4% paraformaldehyde for 15 min at 4°C, washed twice with flow buffer, resuspended in 2% paraformaldehyde and analyzed on a Becton Dickinson LSR II flow cytometer. For indirect staining of CXCR4 and CCR7, DCs were incubated with primary antibody for 1 h at 4°C, washed and incubated with a FITC-conjugated secondary antibody for 30 min at 4°C. Cells were then washed and fixed as described above. 10,000 cells per sample were analyzed. Data analysis was performed using FlowJO software (TreeStar Inc.,

Ashlan, OR, USA). The geometric median fluorescence (MFI) is reported. Gates showing the percentage of FITC-positive cells were set according to the isotype controls.

Endocytosis assay

Endocytosis was measured as the cellular uptake of FITC–dextran and quantified by flow cytometry. DCs (10^5 cells per sample) were incubated in complete medium containing FITC–dextran (1mg/ml) for 30, 60 and 90 min at 4°C or 37°C. After incubation, cells were washed three times with complete medium to remove excess dextran and the uptake of FITC–dextran was determined by flow cytometry. 10,000 cells per sample were analyzed. The MFI of the 4°C controls was less than $8 \pm 1\%$ (average \pm SEM) of the 37°C samples (including both treated and non-treated DCs) in three independent experiments. The MFI of the 4°C controls was subtracted from that of the 37°C samples at each time point and the data were normalized to the MFIs of non-treated DC (= 100%).

mRNA quantification

Individual mRNA transcripts in DCs were quantified using the NanoString nCounter gene expression system (NanoString Technologies Inc., Seattle, WA, USA) using an approach similar to that described by Geiss *et al.* (26). Briefly, 50,000 DCs per condition were lysed in RLT buffer (Qiagen, Valencia, CA, USA) supplemented with β -mercaptoethanol. 10% of the lysates was hybridized for 6 or 16 h with the CodeSet generated by the manufacturer and loaded into the nCounter prep station followed by quantification using the nCounter Digital Analyzer. The nCounter data was normalized in two steps. In the first, we used the positive spiked-in controls provided by the nCounter instrument as per the manufacturer's instructions. Second, we normalized the data to two housekeeping genes, GAPDH and HPRT1.

Quantitative phase microscopy

Immature DCs (day 3) were added to fresh complete medium and mailed overnight from the Research Institute for Children to MIT. Upon receipt, DCs (day 4) were brought up in fresh complete medium and equilibrated at 37°C under 5% CO₂ in a humidified incubator for 2–3 h. Then, DCs were treated with compounds and the cells incubated for an additional 3–6 h. Cells were then collected by centrifugation, washed three times in serum-free RPMI containing 10mM HEPES, pH 7.4, plated on non-coated glass coverslips and incubated overnight. The following day cells were imaged by quantitative phase microscopy (27). Briefly, a diode laser ($\lambda = 532$ nm, Coherent Inc., Santa Clara, CA, USA) was used as illumination source for an inverted microscope (IX71, Olympus Inc., Center Valley, PA, USA) with a 20 \times objective lens (0.5 N.A.), which provides a diffraction-limited transverse resolution of 650 nm. The additional relay optical elements were used to generate interferograms, which were measured with an EMCCD camera (Photonmax 512B, Princeton Instruments Inc., Trenton, NJ, USA). Quantitative phase microscopy employs the principle of laser interferometry and thus measures the full-field optical phase shift induced by the cells that can be translated to cellular thickness maps (28). The instantaneous thickness maps were measured every one second over 12 min and the trajectory of center of mass for each cell was analyzed by custom MatLab® Scripts (The MathWorks, Natick, MA, USA) to retrieve the speed and persistence time. The speed and the persistence time were analyzed by tracking the center of mass of each cell using techniques described previously (29) and the persistence time was calculated using the following equation (30):

$$\langle d^2(t) \rangle = 2n_d \mu \left[t - P \left(1 - e^{-t/P} \right) \right] + 2\gamma$$

Where, n_d = the number of dimensions in which the data were analyzed (=2), μ = random motility coefficient, P = directional persistence time, and γ = mean square positioning error.

Allogeneic MLR

DCs were treated on day 5 of culture with or without 6-Bnz-cAMP, O-Me-cAMP, or 6-Bnz-cAMP and O-Me-cAMP. After 24 h, cells were centrifuged and washed extensively in PBS and medium. DCs (50,000) were cultured with T cells (100,000 per well) in a final volume of 0.2ml in round-bottom 96-well plates for 5 days at 37°C under 5% CO₂ in a humidified incubator. During the last 18 h of culture, cultures were spiked with 1 μ Ci ³H-methyl-thymidine (20Ci/mmol; Perkin Elmer, Waltham, MA, USA). Cells were then harvested onto UniFilter plates using a cell harvester (Perkin Elmer FilterMate Harvester). Radioactivity was counted on a Perkin Elmer TopCount NXT microplate scintillation counter.

Cell viability assay

Immature DCs were treated for 24 h with 6-Bnz-cAMP (100 μ M), O-Me-cAMP (100 μ M), a combination of 6-Bnz-cAMP and O-Me-cAMP (both 100 μ M) or LPS (1 μ g/ml) and then examined for viability using a LIVE/DEAD cell viability assay (Invitrogen). None of the treatments resulted in significant cell death (the average percentage of dead cells in two independent experiments were as follows: non-treated DC 3.64 \pm 0.33%, 6-Bnz-cAMP 1.10 \pm 0.28%, O-Me-cAMP 1.63 \pm 0.53%, 6-Bnz-cAMP and O-Me-cAMP 1.44 \pm 0.21% and LPS 1.34 \pm 0.34%).

Statistical analysis

For the quantitative phase microscopy studies, differences between the means of experimental groups were analyzed by two-tailed Mann-Whitney rank sum test using SigmaPlot software (Systat Software Inc., San Jose, CA, USA). The two-tailed t-test was used to analyze statistical significances between treatment groups in the CREB-phosphorylation studies, the mRNA analysis and in studies comparing cell surface expressed molecules by flow cytometry. Differences were considered significant when $p < 0.05$. In the Transwell cell migration assays, the endocytosis studies and the allogeneic MLR differences between the means of experimental groups were analyzed by single factor ANOVA. For chemotaxis assays: NS, not-statistically significant ($p > 0.05$); a statistical difference between migration to medium and chemotaxis is indicated by * (*, $p < 0.05$; **, $p < 0.01$); a statistical difference between migration of non-treated and treated DCs examined under the same conditions is indicated by # (#, $p < 0.05$; ##, $p < 0.01$). To determine the standard error in the chemotactic index we used the following equation where Med= number of DCs that migrated to medium (random migration) and CC= the number of DCs that migrated to chemokine:

$$\delta y = y \sqrt{\left(\frac{\delta x_{CC}}{x_{CC}}\right)^2 + \left(\frac{\delta x_{Med}}{x_{Med}}\right)^2}$$

Results

Selective activation of PKA, but not Epac, induces the phenotypic maturation of DCs

To investigate whether cAMP signaling via PKA is sufficient to drive the phenotypic maturation of DCs or whether cAMP activation of Epac also plays a role, we used two highly selective cAMP analogs to activate PKA or Epac (6-Bnz-cAMP or O-Me-cAMP, respectively). First, we confirmed that human monocyte-derived DCs express Epac1 by immunoblot (data not shown). These data agree with previous reports that Epac1 is

expressed in human primary leukocytes, platelets and CD34-positive hematopoietic cells (31). Next, immature DCs were treated with the PKA or Epac agonists and expression of the co-stimulatory molecules CD80 and CD86 was examined by flow cytometry. We also examined the expression of CD83, a marker expressed by mature DCs (32). We found that PKA, but not Epac, increased DC expression of all three molecules (Figure 1). To confirm these results, we showed in a separate experiment that the PKA agonist increased DC expression of co-stimulatory molecules and CD83 to a similar extent as that observed for DCs treated with the potent cAMP-elevating stimulus cholera toxin (CT), the phosphodiesterase-resistant cAMP analog dibutyryl cAMP (db-cAMP) and a phosphodiesterase inhibitor (IBMX) (Supplemental Figure 1). These data suggest that cAMP activation of PKA, but not Epac, induces the phenotypic maturation of DCs.

To address whether crosstalk between the PKA and Epac signaling pathways regulates DC maturation, DCs were treated simultaneously with the PKA and Epac agonists. In addition to increasing the cell surface expression of co-stimulatory molecules and CD83, PKA increased the expression of MHC class II (Figure 2A, compare grey histograms with bold line histograms). When the agonists were added together, Epac partially reduced the expression of CD80, CD83, CD86 and MHC class II (Figure 2A, compare bold line histograms with thin line histograms). In contrast, the Epac agonist alone had no effect on the expression of any of these molecules (data not shown).

We next confirmed these results in ten independent experiments using DCs derived from different donors. PKA, but not Epac, significantly increased the cell surface expression of MHC class II, CD80, CD83 and CD86 (Supplemental Figure 2). When the agonists were added simultaneously, Epac significantly reduced DC expression of MHC class II, CD80 and CD86. This trend was also true for CD83 although these data were not significantly different. To further validate these results, we use digital mRNA profiling to quantify transcripts encoding CD80, CD83 and CD86. DCs treated with the PKA agonist for 6 h showed a significant increase in transcripts for all three molecules relative to non-treated DCs (Figure 2B). In contrast, the Epac agonist had no effect on transcript levels. When DCs were treated simultaneously with the PKA and Epac agonists, Epac reduced the number of transcripts for CD80 and CD83 after 6 h of incubation and significantly reduced the level of CD86 transcripts after 16 h of incubation (Figure 2B). These data suggest that PKA-Epac crosstalk regulates the expression of CD80, CD83 and CD86 at the level of transcription. Taken together, these data demonstrate that the selective activation of PKA is sufficient to induce the phenotypic maturation of DCs and that Epac antagonizes this effect.

Crosstalk between PKA and Epac regulates DC chemotaxis to the CXCR4 ligand CXCL12

DC maturation and chemotaxis are intimately linked (33,34). Therefore, we next tested whether PKA and Epac signaling could regulate DC chemotaxis to CXCL12. DCs were treated with the PKA or Epac agonists for 24 h and then examined for chemotaxis using Transwell cell migration assays. The PKA agonist stimulated robust chemotaxis to CXCL12 (Figure 3A, black bars). This effect was dose-dependent and comparable to that observed for DCs treated with CT or db-cAMP (Supplemental figure 3A, black bars and data not shown). In contrast, the Epac agonist failed to simulate DC chemotaxis (Figure 3A and Supplemental figure 3A, black bars). The chemotactic index, a ratio of the number of DCs that migrated in response to chemokine to the number of DCs that migrated to medium, shows that both the PKA agonist and CT induced a strong chemotactic response to CXCL12 (Figure 3B and Supplemental figure 3B). A novel observation was that activation of PKA induced DC migration in the absence of chemokine (random migration) (Figure 3A, white bars and Supplemental figure 3A, white bars). Like the PKA agonist, both CT and db-cAMP induced random migration (Supplemental figure 3A, white bars and data not shown). In contrast, the Epac agonist failed to stimulate random migration. These results suggest that cAMP

signaling via PKA increases the intrinsic capacity of DCs to migrate in the absence of a chemical cue.

We next examined whether crosstalk between the PKA and Epac signaling pathways regulates DC chemotaxis and random migration. DCs treated with the PKA and Epac agonists at the same time exhibited significantly reduced chemotaxis to CXCL12 when compared with DCs treated with the PKA agonist in the presence or absence of DMSO (vehicle control for the Epac agonist) (Figure 3A, black bars). Incubation of DCs with both agonists, however, did not affect random migration (Figure 3A, white bars). The chemotactic index clearly demonstrates that Epac interfered with the ability of PKA to induce DC chemotaxis to CXCL12 (Figure 3B). This set of data shows that Epac interferes with the ability of PKA to stimulate DC chemotaxis to CXCL12 but has no effect on PKA-mediated random migration.

In addition to random migration in the absence of a chemical cue, cells may exhibit non-directed migration in a uniform concentration of a chemokine, a process termed chemokinesis. We next compared the effect of PKA and Epac on DC chemokinesis in uniform concentrations of CXCL12. The PKA agonist stimulated all three forms of migration: chemokinesis, random migration and chemotaxis (Figure 3C). In contrast, the Epac agonist failed to stimulate any form of migration. When DCs were co-incubated with the Epac and PKA agonists, Epac reduced chemotaxis to CXCL12 but failed to inhibit random migration or chemokinesis (Figure 3C). DCs incubated with the PKA agonist in the presence of DMSO exhibited no significant differences in chemotaxis, random migration or chemokinesis when compared with DCs treated with the PKA agonist alone indicating that the effect of the Epac agonist on PKA-mediated chemotaxis cannot be explained by a non-specific effect of DMSO. Taken together, these data show that Epac inhibits PKA-mediated chemotaxis to CXCL12 without affecting random migration or chemokinesis.

PKA weakly stimulates DC chemotaxis to CCL21

We next examined the effect of cAMP signaling on DC chemotaxis to the CCR7 ligand CCL21. Dibutyryl-cAMP stimulated robust DC chemotaxis to CCL21 in a manner similar to that observed for LPS, a cAMP-independent stimulus known to induce migration to CCL21 (Figure 4A and B). In contrast, the PKA agonist failed to stimulate chemotaxis to CCL21 while inducing random migration (Figure 4A, compare black with white bars). Treatment of DCs with a 5-fold greater concentration of the PKA agonist also failed to stimulate significant DC chemotaxis to CCL21 (data not shown). As shown for CXCL12, the Epac agonist failed to stimulate DC chemotaxis to CCL21. Furthermore, incubation of DCs with the PKA and Epac agonists simultaneously had no effect on chemotaxis. To test whether the PKA agonist could induce DC chemotaxis but with delayed kinetics, DCs were treated the PKA agonist for 48 h. At the later time point, PKA induced chemotaxis to CCL21 although the response was much less robust when compared with DCs treated with db-cAMP or LPS for 48 h (Supplemental Figure 4). When DCs were incubated with both agonists simultaneously, chemotaxis to CCL21 was reduced when compared with DCs incubated with the PKA agonist alone. However, DMSO also reduced the ability of the PKA agonist to induce DC chemotaxis suggesting that prolonged incubation with DMSO may have a non-specific effect on DC migration. This set of data suggests that PKA signaling differentially regulates DC chemotaxis to the CXCR4 and CCR7 ligands.

PKA regulates the speed and persistence time of DC random migration

Next, we used quantitative phase microscopy to examine the effect of PKA activation on DC random migration. Non-treated and CT-treated DCs were cultured on glass coverslips and DC migration in medium was imaged every second over a 12 min interval. The speed ($\mu\text{m}/$

min) and the persistence time (time in seconds in which DCs remained on a given course before changing direction by an angle of $\geq 60^\circ$) were analyzed by tracking the center of mass of individual cells. CT significantly increased the speed of CCL21 but induced random migration over that of non-treated DCs ($\sim 5 \mu\text{m}/\text{min}$ versus $\sim 2.5 \mu\text{m}/\text{min}$, Supplemental figure 5A and C and Movies 1–4). CT treatment also increased the persistence time of DC migration compared with non-treated DCs (~ 7.5 seconds versus ~ 2.5 seconds, Supplemental figure 5B and D). Consistent with an increased speed of random migration, CT induced the dynamic formation of membrane protrusions, retractions and membrane ruffling events in DCs that was not observed in non-treated DCs (Movies 1–4 and data not shown). This set of data shows that CT-treated DCs migrate faster and remain on a given path for a longer duration of time before changing direction when compared with non-treated DCs.

Using the same approach we next compared the random migration of DCs treated with the PKA agonist, CT, db-cAMP, IBMX or LPS. Consistent with the Transwell cell migration data, the PKA agonist and CT significantly increased the speed of DC random migration when compared with non-treated or LPS-treated DCs (Supplemental figure 5C). This was also true for DCs treated with db-cAMP or IBMX. In addition, the PKA agonist, CT, db-cAMP and IBMX also increased the persistence time of DC random migration (Supplemental figure 5D). While LPS did not affect the speed of migration it did increase the persistence of DC migration although less effectively than did the other compounds. Taken together, these data show that PKA signaling is sufficient to increase the speed and persistence time of DC random migration.

Crosstalk between the PKA and Epac signaling pathways regulate DC expression of CXCR4

To determine whether Epac signaling reduced DC chemotaxis to CXCL12 by down-regulating CXCR4 expression, we measured DC cell surface expression of CXCR4 by flow cytometry. We found that immature DCs expressed only low levels of CXCR4 on the cell surface (Figure 5A, thin line histogram). Consistent with the ability of the PKA to induce DC chemotaxis to CXCL12, the PKA agonist increased DC expression of CXCR4 (Figure 5A, bold line histogram). In line with our observation that Epac failed to induce DC chemotaxis to CXCL12, the Epac agonist had no effect on DC expression of CXCR4 (Figure 5A, dotted line histogram). When DCs were incubated with the agonists simultaneously, the Epac agonist decreased CXCR4 expression (Figure 5A, compare the bold line histogram with the grey histogram). This was also true when DCs were co-incubated with the Epac agonist and CT (data not shown). None of the treatments had any effect on the staining pattern of the isotype control antibody (Figure 5B). To confirm this result, we analyzed the effect of PKA and Epac on the expression of CXCR4 using DCs prepared from different donors (Figure 5C). These data show that the PKA agonist significantly increased CXCR4 expression on the DC cell surface relative to non-treated DCs and that the Epac signaling had no effect on the expression of CXCR4. Epac did, however, reduce CXCR4 expression in DCs incubated with both agonists at the same time (Figure 5C). These data show that Epac activation interferes with PKA-mediated up-regulation of CXCR4 expression and are in line with the effects of these agonists on DC chemotaxis to CXCL12.

To further validate these data, we quantified RNA transcripts for the two known isoforms of CXCR4 using digital mRNA profiling. We also used this technique to examine differences in transcripts encoding CXCR7, a newly identified second chemokine receptor for CXCL12 (35,36). Incubation of DCs with the PKA agonist induced an increase in CXCR4 mRNA (both isoforms 1 and 2) at 6 and 16 h (Figure 5D and E). In contrast, the Epac agonist had no effect on CXCR4 transcription. Importantly, Epac significantly reduced CXCR4 mRNA levels in DCs incubated with both agonists for 6 or 16 h. We also found that PKA, but not

Epac, increased the abundance of CXCR7 transcripts at both time points and that Epac reduced the PKA-dependent increase in CXCR7 mRNA levels (Figure 5F). Taken together, this set of data shows that PKA signaling is sufficient to induce CXCR4 and CXCR7 mRNA transcription and that Epac suppresses this effect.

We also examined the effect of PKA and Epac activation on DC expression of CCR7. Immature DCs expressed low levels of CCR7 and the PKA and Epac agonists added separately or together had no effect on CCR7 expression levels (Supplemental Figure 6). These data are consistent with the inability of PKA to induce DC chemotaxis to CCL21. In contrast, LPS significantly increased CCR7 expression and this is in line with our observation that LPS stimulated DC chemotaxis to CCL21. Treatment of DCs with the PKA agonist for a 48 h interval induced only a small increase in CCR7 and this was not affected by incubation of DCs with the Epac agonist (data not shown). These data suggest that PKA regulates DC expression of CXCR4 but has a minimal effect on expression of the CCL21 ligand CCR7.

Epac signaling reduces PKA-mediated phosphorylation of CREB

To test the possibility that Epac signaling interferes with PKA phosphorylation of the transcription factor CREB, a known downstream target of PKA, we incubated DCs with the PKA agonist or LPS for 30 min and detected phosphorylated CREB and total CREB by immunoblot. Both the PKA agonist and LPS induced CREB phosphorylation and the extent of phosphorylation was dependent on the dose of the PKA agonist (Figure 6A and B). Next, DCs were incubated with LPS, the PKA or Epac agonists or both agonists together and cells were analyzed for CREB phosphorylation. Both the PKA agonist and LPS induced CREB phosphorylation while the Epac agonist had no effect on CREB phosphorylation (Figure 6C and D). However, Epac significantly reduced PKA-mediated phosphorylation of CREB. Data from four separate experiments show that Epac reduced the phospho-CREB signal by $20 \pm 5\%$ (average \pm SEM; Figure 6E). The CXCR4 gene promoter contains a cAMP-responsive element and it has been shown that PKA up-regulates CXCR4 expression in DCs (37). Thus, this set of data provides a molecular basis for the reduced expression of CXCR4 and impaired chemotaxis to CXCL12 observed after simultaneous activation of PKA and Epac in DCs.

PKA-Epac crosstalk regulates DC endocytosis

Another hallmark of mature DCs is decreased antigen uptake via endocytosis. Thus, we examined whether cAMP signaling through PKA could down-regulate DC uptake of FITC-dextran over a time course of 90 min. Immature DCs actively took up FITC-dextran at each time point and uptake was significantly reduced when DCs were induced to mature by incubation with LPS for 24 h (Figure 7A). The PKA agonist also reduced DC uptake of dextran at each time point while the Epac agonist had no significant effect on endocytosis (Figure 7A). When DCs were incubated with the PKA and Epac agonists at the same time, Epac interfered with the ability of the PKA agonist to reduce endocytosis and this effect could not be explained by the presence of DMSO (Figure 7A). When data from all three time points were compiled, LPS-treated DCs took up $\sim 61\%$ less dextran when compared with non-treated immature DCs (Figure 7B), demonstrating that LPS-induced DC maturation correlated with a decrease in endocytic activity. The PKA agonist also induced DC maturation as evidenced by a $\sim 50\%$ decrease in dextran uptake when compared with immature DCs. Finally, treatment of DCs with both agonists reduced endocytosis by only $\sim 26\%$ while treatment with the Epac agonist alone only slightly reduced endocytosis ($\sim 11\%$). These data show that Epac interferes with the ability of the PKA to induce DC maturation.

PKA-Epac crosstalk regulates DC cytokine production

To further examine PKA-Epac regulation of DC function, we used mRNA profiling to quantify the effect of PKA and Epac signaling on cytokine production. When compared with non-treated immature DCs, DCs treated with the PKA agonist exhibited reduced levels of mRNA transcripts encoding TNF- α , TGF- β , IL-18 and IL-10 (Figure 8A-H). The Epac agonist alone had no effect on the level of transcripts encoding these cytokines. When DCs were incubated with both agonists, Epac had no effect on TNF- α and TGF- β mRNA levels, but partially reversed the inhibitory effect of PKA on IL-18 and IL-10 mRNA levels following 6 h of incubation. None of the treatments had any effect on the already low levels of IL-12 mRNA in immature DCs (data not shown). Taken together, these data suggest that PKA suppresses cytokine production by DCs and that Epac partially reverses this effect.

PKA-Epac crosstalk regulates DC activation of T cells

Finally, we tested whether PKA-Epac crosstalk could regulate DC activation of allogeneic T cells. DCs were treated with the PKA or Epac agonists added separately or together and incubated with allogeneic T cells. The PKA agonist enhanced the ability of DCs to stimulate T cell proliferation while the Epac agonist had no effect on T cell proliferation (Figure 9). When DCs were cultured with both agonists, T cell proliferation was reduced when compared with DCs activated with the PKA agonist alone. This set of data shows that PKA enhances DC activation of T cells and that Epac signaling interferes with this effect.

Discussion

The cAMP-dependent signaling pathways that regulate DC maturation remain to be completely defined. This led us to investigate whether cAMP signaling via PKA is sufficient to drive maturation or whether cAMP activation of Epac is also involved. To address this question, we used cAMP analogs specific for PKA or Epac to discriminate the effect of these signaling pathways on the maturation of human monocyte-derived DCs. The experiments presented here show that selective activation of PKA stimulates DC maturation. In contrast, Epac signaling has no effect on maturation. However, when both pathways are activated simultaneously, Epac antagonizes the effect of PKA on the phenotypic maturation and function of DCs. Specifically, we found that the cell surface expression of MHC class II, co-stimulatory molecules, the maturation marker CD83 and the chemokine receptor CXCR4 was reduced when DCs were treated with the PKA and Epac agonists at the same time. Epac also interfered with PKA activation of CREB suggesting that PKA-Epac crosstalk may converge at the level of transcription to regulate DC maturation. Further, Epac antagonized the effect of PKA on DC function. Epac partially reversed the effect of PKA on endocytosis, chemotaxis to CXCL12, cytokine production and T cell activation. These findings suggest that the net effect of cAMP signaling is not simply dictated by the action of PKA or Epac alone, but involves a complex integration of the two signaling pathways.

A novel finding of this study was that in addition to up-regulating CXCR4, PKA activation increased DC transcription of CXCR7. While CXCR4 and CXCL12 were once thought to form a monogamous pair, CXCR7 was recently identified as a second chemokine receptor for CXCL12 (35,36,38–44). Unlike other chemokine receptors, CXCR7 does not stimulate chemotaxis (36). Rather, CXCR7 is thought to belong to the atypical chemokine receptor family that play a role in scavenging or altering the localization of chemokines via binding and/or internalizing the chemokines without inducing signal transduction (45). A prevailing theory is that CXCR7 may function to scavenge CXCL12 at the trailing edge of migrating cells thus creating a local chemokine gradient around the cell to maintain the directionality of migration (46–50). Interestingly, we also found that PKA increased the transcription of two isoforms of CXCR4 and that Epac partially antagonized this effect. The significance of

PKA-mediated up-regulation of both CXCR4 isoforms and CXCR7 for DC chemotaxis to CXCL12 remains to be elucidated.

An unexpected finding of this study was that DCs treated with the PKA agonist migrated strongly to CXCL12 but poorly to CCL21. In humans, it is currently not known whether CCR7 is the dominant chemokine receptor for directing DC migration to lymph nodes or whether CXCR4 also plays a role. In murine DCs, both CCR7 and CXCR4 direct migration to lymphoid tissues (38,41,42,51–59). CCR7-deficient mice and *plt/plt* mutant mice (which lack both CCR7 ligands CCL19 and CCL21) exhibit a severe defect in DC migration from the skin to the draining lymph nodes. The observed defect is still incomplete, suggesting the involvement of another chemokine receptor. Indeed, CXCR4 is required for the migration of murine DCs (both Langerhans cells and dermal DCs) to the skin-draining lymph nodes (60). In humans, CXCR4 is required for the chemotaxis of DCs from the epidermis to the dermis (54). CXCR4 also functions synergistically with CXCR3 to induce the migration of human plasmacytoid DCs to lymph nodes (61). In addition to regulating chemotaxis, CXCL12 promotes murine DC survival and maturation (62). Our preliminary results show that CXCL12 increases human DC expression of MHC class II and co-stimulatory molecules (our unpublished observation, J.G. and B.L.D.). Thus, PKA-dependent up-regulation of CXCR4 may augment both DC maturation and homing to lymphoid tissues.

DCs exhibit non-directional migration in the absence of chemical cues (random migration) and in symmetrical concentrations of chemoattractants (chemokinesis). We found that PKA activation induced both forms of migration. It is thought that random migration may function to prime DC chemotaxis by sensitizing the chemotaxis machinery (63,64). For example, PKA signaling has been shown to lower the threshold for chemokine receptor detection of chemokines and facilitate cell migration in response to distant or suboptimal chemokine signals (65). Another role for non-directional migration may be to increase the frequency of DC contacts with T cells within the crowded confines of lymphoid tissues where chemokine gradients may play a less important role in directing cell migration (66,67). Our data show that while both the PKA agonist and CT induced DC random migration, only the PKA agonist stimulated chemokinesis. One possibility to explain this result is that the PKA agonist may activate PKA more potently than CT. We also found that Epac signaling failed to stimulate DC random migration and chemokinesis. And, although Epac partially inhibited the chemotaxis of PKA-treated DCs, Epac had no effect on the ability of PKA to induce DC random migration or chemokinesis. These results suggest that the cAMP-dependent mechanisms that direct chemotaxis, random migration and chemokinesis may be differentially regulated in DCs.

In most cases, the ultimate consequence of DC maturation for the immune response is T cell activation. T cell differentiation into Th1, Th2, Th17 or T regulatory effectors is strongly influenced by the pattern of cytokines released by DCs during antigen presentation. We found that transcription of TNF- α , TGF- β , IL-18 and IL-10 was suppressed in DCs treated with the PKA agonist. This result is in line with the observation that cAMP-elevating bacterial toxins such as CT, the *E. coli* heat-labile enterotoxin (LT), pertussis toxin and adenylate cyclase toxin activate human monocyte-derived DCs and inhibit cytokine production (68,69). CT and LT are potent mucosal adjuvants that act on DCs to promote T cell responses to co-delivered protein antigens (18,70–74). Despite the inhibitory effect of PKA on cytokine expression, we found that PKA-treated DCs stimulated allogeneic T cell proliferation *in vitro*. While Epac had no effect on cytokine transcript levels, it partially reversed the inhibitory effect of PKA on the transcription of IL-18 and IL-10. Epac also diminished the capacity of PKA-activated DCs to stimulate T cell proliferation. Thus, Epac may function as a “molecular break” to attenuate the magnitude of PKA signaling to prevent excessive T cell activation. Our data suggest that PKA-Epac crosstalk may converge at the

level of transcription to regulate DC maturation and function. In support of this idea, we show that Epac interferes with PKA phosphorylation of CREB, and others have shown that Epac regulates the activity of the C/EBP family of transcription factors (75,76). How cAMP signaling regulates transcription may depend on the strength, duration and timing of PKA and Epac activation. These signals must also be integrated with signaling events initiated by DC interaction with pathogen-associated molecules, such as TLR ligands, as well as with signaling molecules that originate from neighboring cells (77).

In summary, the results of this study have important implications for DC-based cancer vaccines. A current focus is on the development of novel stimuli for the *ex vivo* conditioning of DCs to promote their maturation and migration to lymph nodes for T cell priming. Future studies will be required to determine whether stimuli that activate PKA generate mature, immunogenic DCs capable of activating T cells *in vivo* and conversely, whether stimuli that target Epac generate tolerogenic DCs capable of attenuating allergic and autoimmune disease (6,78).

Supplementary Material

Refer to Web version on PubMed Central for supplementary material.

Acknowledgments

We thank Ms. Alexandra Baker for excellent technical assistance. This manuscript is dedicated in memory of Dr. Martha Aiken a wonderful scientist and friend.

References

1. Steinman RM, Bonifaz L, Fujii S, Liu K, Bonnyay D, Yamazaki S, Pack M, Hawiger D, Iyoda T, Inaba K, Nussenzweig MC. The innate functions of dendritic cells in peripheral lymphoid tissues. *Adv Exp Med Biol.* 2005; 560:83–97. [PubMed: 15932024]
2. Mellman I, Steinman RM. Dendritic cells: specialized and regulated antigen processing machines. *Cell.* 2001; 106:255–258. [PubMed: 11509172]
3. Sallusto F, Schaerli P, Loetscher P, Schaniel C, Lenig D, Mackay CR, Qin S, Lanzavecchia A. Rapid and coordinated switch in chemokine receptor expression during dendritic cell maturation. *Eur J Immunol.* 1998; 28:2760–2769. [PubMed: 9754563]
4. Hawiger D, Inaba K, Dorsett Y, Guo M, Mahnke K, Rivera M, Ravetch JV, Steinman RM, Nussenzweig MC. Dendritic cells induce peripheral T cell unresponsiveness under steady state conditions in vivo. *J Exp Med.* 2001; 194:769–779. [PubMed: 11560993]
5. Steinman RM, Hawiger D, Liu K, Bonifaz L, Bonnyay D, Mahnke K, Iyoda T, Ravetch J, Dhodapkar M, Inaba K, Nussenzweig M. Dendritic cell function in vivo during the steady state: a role in peripheral tolerance. *Ann N Y Acad Sci.* 2003; 987:15–25. [PubMed: 12727620]
6. Dhodapkar MV, Steinman RM, Krasovsky J, Munz C, Bhardwaj N. Antigen-specific inhibition of effector T cell function in humans after injection of immature dendritic cells. *J Exp Med.* 2001; 193:233–238. [PubMed: 11208863]
7. Finke LH, Wentworth K, Blumenstein B, Rudolph NS, Levitsky H, Hoos A. Lessons from randomized phase III studies with active cancer immunotherapies--outcomes from the 2006 meeting of the Cancer Vaccine Consortium (CVC). *Vaccine.* 2007; 25(Suppl 2):B97–B109. [PubMed: 17916465]
8. Finn OJ. Cancer vaccines: between the idea and the reality. *Nat Rev Immunol.* 2003; 3:630–641. [PubMed: 12974478]
9. Nestle FO, Aljagic S, Gilliet M, Sun Y, Grabbe S, Dummer R, Burg G, Schadendorf D. Vaccination of melanoma patients with peptide- or tumor lysate-pulsed dendritic cells. *Nat Med.* 1998; 4:328–332. [PubMed: 9500607]

10. Nestle FO, Banchereau J, Hart D. Dendritic cells: On the move from bench to bedside. *Nat Med*. 2001; 7:761–765. [PubMed: 11433329]
11. Thurner B, Haendle I, Roder C, Dieckmann D, Keikavoussi P, Jonuleit H, Bender A, Maczek C, Schreiner D, von den Driesch P, Brocker EB, Steinman RM, Enk A, Kampgen E, Schuler G. Vaccination with mage-3A1 peptide-pulsed mature, monocyte-derived dendritic cells expands specific cytotoxic T cells and induces regression of some metastases in advanced stage IV melanoma. *J Exp Med*. 1999; 190:1669–1678. [PubMed: 10587357]
12. Rosenberg SA, Yang JC, Restifo NP. Cancer immunotherapy: moving beyond current vaccines. *Nat Med*. 2004; 10:909–915. [PubMed: 15340416]
13. Li K, Anderson KJ, Peng Q, Noble A, Lu B, Kelly AP, Wang N, Sacks SH, Zhou W. Cyclic AMP plays a critical role in C3a-receptor-mediated regulation of dendritic cells in antigen uptake and T-cell stimulation. *Blood*. 2008; 112:5084–5094. [PubMed: 18812470]
14. Wilkin F, Duhant X, Bruyns C, Suarez-Huerta N, Boeynaems JM, Robaye B. The P2Y11 receptor mediates the ATP-induced maturation of human monocyte-derived dendritic cells. *J Immunol*. 2001; 166:7172–7177. [PubMed: 11390464]
15. Goyarts E, Matsui M, Mammone T, Bender AM, Wagner JA, Maes D, Granstein RD. Norepinephrine modulates human dendritic cell activation by altering cytokine release. *Exp Dermatol*. 2008; 17:188–196. [PubMed: 18205818]
16. Maldonado-Arocho FJ, Bradley KA. Anthrax edema toxin induces maturation of dendritic cells and enhances chemotaxis towards macrophage inflammatory protein 3beta. *Infect Immun*. 2009; 77:2036–2042. [PubMed: 19273556]
17. Delneste Y, Herbault N, Galea B, Magistrelli G, Bazin I, Bonnefoy JY, Jeannin P. Vasoactive intestinal peptide synergizes with TNF-alpha in inducing human dendritic cell maturation. *J Immunol*. 1999; 163:3071–3075. [PubMed: 10477571]
18. Bagley KC, Abdelwahab SF, Tuskan RG, Lewis GK. Cholera toxin indirectly activates human monocyte-derived dendritic cells in vitro through the production of soluble factors, including prostaglandin E(2) and nitric oxide. *Clin Vaccine Immunol*. 2006; 13:106–115. [PubMed: 16426007]
19. Luft T, Jefford M, Luetjens P, Toy T, Hochrein H, Masterman KA, Maliszewski C, Shortman K, Cebon J, Maraskovsky E. Functionally distinct dendritic cell (DC) populations induced by physiologic stimuli: prostaglandin E(2) regulates the migratory capacity of specific DC subsets. *Blood*. 2002; 100:1362–1372. [PubMed: 12149219]
20. de Rooij J, Zwartkruis FJ, Verheijen MH, Cool RH, Nijman SM, Wittinghofer A, Bos JL. Epac is a Rap1 guanine-nucleotide-exchange factor directly activated by cyclic AMP. *Nature*. 1998; 396:474–477. [PubMed: 9853756]
21. Kawasaki H, Springett GM, Mochizuki N, Toki S, Nakaya M, Matsuda M, Housman DE, Graybiel AM. A family of cAMP-binding proteins that directly activate Rap1. *Science*. 1998; 282:2275–2279. [PubMed: 9856955]
22. Cheng X, Ji Z, Tsalkova T, Mei F. Epac and PKA: a tale of two intracellular cAMP receptors. *Acta Biochim Biophys Sin (Shanghai)*. 2008; 40:651–662. [PubMed: 18604457]
23. Dao KK, Teigen K, Kopperud R, Hodneland E, Schwede F, Christensen AE, Martinez A, Doskeland SO. Epac1 and cAMP-dependent protein kinase holoenzyme have similar cAMP affinity, but their cAMP domains have distinct structural features and cyclic nucleotide recognition. *J Biol Chem*. 2006; 281:21500–21511. [PubMed: 16728394]
24. Enserink JM, Christensen AE, de Rooij J, van Triest M, Schwede F, Genieser HG, Doskeland SO, Blank JL, Bos JL. A novel Epac-specific cAMP analogue demonstrates independent regulation of Rap1 and ERK. *Nat Cell Biol*. 2002; 4:901–906. [PubMed: 12402047]
25. Christensen AE, Selheim F, de Rooij J, Dremier S, Schwede F, Dao KK, Martinez A, Maenhaut C, Bos JL, Genieser HG, Doskeland SO. cAMP analog mapping of Epac1 and cAMP kinase. Discriminating analogs demonstrate that Epac and cAMP kinase act synergistically to promote PC-12 cell neurite extension. *J Biol Chem*. 2003; 278:35394–35402. [PubMed: 12819211]
26. Geiss GK, Bumgarner RE, Birditt B, Dahl T, Dowidar N, Dunaway DL, Fell HP, Ferree S, George RD, Grogan T, James JJ, Maysuria M, Mitton JD, Oliveri P, Osborn JL, Peng T, Ratcliffe AL,

- Webster PJ, Davidson EH, Hood L, Dimitrov K. Direct multiplexed measurement of gene expression with color-coded probe pairs. *Nat Biotechnol.* 2008; 26:317–325. [PubMed: 18278033]
27. Park Y, Popescu G, Badizadegan K, Dasari RR, Feld MS. Diffraction phase and fluorescence microscopy. *Opt Express.* 2006; 14:8263–8268. [PubMed: 19529201]
28. Popescu G, Park Y, Lue N, Best-Popescu C, Deflores L, Dasari RR, Feld MS, Badizadegan K. Optical imaging of cell mass and growth dynamics. *Am J Physiol Cell Physiol.* 2008; 295:C538–544. [PubMed: 18562484]
29. Barer R. Determination of dry mass, thickness, solid and water concentration in living cells. *Nature.* 1953; 172:1097–1098. [PubMed: 13111263]
30. Burgess BT, Myles JL, Dickinson RB. Quantitative analysis of adhesion-mediated cell migration in three-dimensional gels of RGD-grafted collagen. *Ann Biomed Eng.* 2000; 28:110–118. [PubMed: 10645794]
31. Lorenowicz MJ, van Gils J, de Boer M, Hordijk PL, Fernandez-Borja M. Epac1-Rap1 signaling regulates monocyte adhesion and chemotaxis. *J Leukoc Biol.* 2006; 80:1542–1552. [PubMed: 16940330]
32. Zhou LJ, Tedder TF. Human blood dendritic cells selectively express CD83, a member of the immunoglobulin superfamily. *J Immunol.* 1995; 154:3821–3835. [PubMed: 7706722]
33. Foti M, Granucci F, Aggularo D, Liboi E, Luini W, Minardi S, Mantovani A, Sozzani S, Ricciardi-Castagnoli P. Upon dendritic cell (DC) activation chemokines and chemokine receptor expression are rapidly regulated for recruitment and maintenance of DC at the inflammatory site. *Int Immunol.* 1999; 11:979–986. [PubMed: 10360972]
34. Randolph GJ, Sanchez-Schmitz G, Angeli V. Factors and signals that govern the migration of dendritic cells via lymphatics: recent advances. *Springer Semin Immunopathol.* 2005; 26:273–287. [PubMed: 15338191]
35. Balabanian K, Lagane B, Infantino S, Chow KY, Harriague J, Moepps B, Arenzana-Seisdedos F, Thelen M, Bachelier F. The chemokine SDF-1/CXCL12 binds to and signals through the orphan receptor RDC1 in T lymphocytes. *J Biol Chem.* 2005; 280:35760–35766. [PubMed: 16107333]
36. Burns JM, Summers BC, Wang Y, Melikian A, Berahovich R, Miao Z, Penfold ME, Sunshine MJ, Littman DR, Kuo CJ, Wei K, McMaster BE, Wright K, Howard MC, Schall TJ. A novel chemokine receptor for SDF-1 and I-TAC involved in cell survival, cell adhesion, and tumor development. *J Exp Med.* 2006; 203:2201–2213. [PubMed: 16940167]
37. Gagliardi MC, De Magistris MT. Maturation of human dendritic cells induced by the adjuvant cholera toxin: role of cAMP on chemokine receptor expression. *Vaccine.* 2003; 21:856–861. [PubMed: 12547594]
38. Martín-Fontecha A, Sebastiani S, Hopken UE, Ugucioni M, Lipp M, Lanzavecchia A, Sallusto F. Regulation of dendritic cell migration to the draining lymph node: impact on T lymphocyte traffic and priming. *J Exp Med.* 2003; 198:615–621. [PubMed: 12925677]
39. Sallusto F, Lanzavecchia A. Understanding dendritic cell and T-lymphocyte traffic through the analysis of chemokine receptor expression. *Immunol Rev.* 2000; 177:134–140. [PubMed: 11138771]
40. Sallusto F, Mackay CR, Lanzavecchia A. The role of chemokine receptors in primary, effector, and memory immune responses. *Annu Rev Immunol.* 2000; 18:593–620. [PubMed: 10837070]
41. Caux C, Vanbervliet B, Massacrier C, Ait-Yahia S, Vaure C, Chemin K, Dieu N, Vicari McA. Regulation of dendritic cell recruitment by chemokines. *Transplantation.* 2002; 73:S7–11. [PubMed: 11810053]
42. Caux C, Ait-Yahia S, Chemin K, de Bouteiller O, Dieu-Nosjean MC, Homey B, Massacrier C, Vanbervliet B, Zlotnik A, Vicari A. Dendritic cell biology and regulation of dendritic cell trafficking by chemokines. *Springer Semin Immunopathol.* 2000; 22:345–369. [PubMed: 11155441]
43. Forster R, Schubel A, Breitfeld D, Kremmer E, Renner-Muller I, Wolf E, Lipp M. CCR7 coordinates the primary immune response by establishing functional microenvironments in secondary lymphoid organs. *Cell.* 1999; 99:23–33. [PubMed: 10520991]

44. Infantino S, Moepps B, Thelen M. Expression and regulation of the orphan receptor RDC1 and its putative ligand in human dendritic and B cells. *J Immunol.* 2006; 176:2197–2207. [PubMed: 16455976]
45. Comerford I, Litchfield W, Harata-Lee Y, Nibbs RJ, McColl SR. Regulation of chemotactic networks by ‘atypical’ receptors. *Bioessays.* 2007; 29:237–247. [PubMed: 17295321]
46. Boldajipour B, Mahabaleswar H, Kardash E, Reichman-Fried M, Blaser H, Minina S, Wilson D, Xu Q, Raz E. Control of chemokine-guided cell migration by ligand sequestration. *Cell.* 2008; 132:463–473. [PubMed: 18267076]
47. Dambly-Chaudiere C, Cubedo N, Ghysen A. Control of cell migration in the development of the posterior lateral line: antagonistic interactions between the chemokine receptors CXCR4 and CXCR7/RDC1. *BMC Dev Biol.* 2007; 7:23. [PubMed: 17394634]
48. Knaut H, Schier AF. Clearing the path for germ cells. *Cell.* 2008; 132:337–339. [PubMed: 18267065]
49. Perlin JR, Talbot WS. Signals on the move: chemokine receptors and organogenesis in zebrafish. *Sci STKE.* 2007; 2007:pe45. [PubMed: 17712137]
50. Valentin G, Haas P, Gilmour D. The chemokine SDF1a coordinates tissue migration through the spatially restricted activation of Cxcr7 and Cxcr4b. *Curr Biol.* 2007; 17:1026–1031. [PubMed: 17570670]
51. Bai Z, Hayasaka H, Kobayashi M, Li W, Guo Z, Jang MH, Kondo A, Choi BI, Iwakura Y, Miyasaka M. CXC chemokine ligand 12 promotes CCR7-dependent naive T cell trafficking to lymph nodes and Peyer’s patches. *J Immunol.* 2009; 182:1287–1295. [PubMed: 19155474]
52. Mori S, Nakano H, Aritomi K, Wang CR, Gunn MD, Kakiuchi T. Mice lacking expression of the chemokines CCL21-ser and CCL19 (plt mice) demonstrate delayed but enhanced T cell immune responses. *J Exp Med.* 2001; 193:207–218. [PubMed: 11148224]
53. Junt T, Nakano H, Dumrese T, Kakiuchi T, Odermatt B, Zinkernagel RM, Hengartner H, Ludewig B. Antiviral immune responses in the absence of organized lymphoid T cell zones in plt/plt mice. *J Immunol.* 2002; 168:6032–6040. [PubMed: 12055211]
54. Ouwehand K, Santegoets SJ, Bruynzeel DP, Scheper RJ, de Gruijl TD, Gibbs S. CXCL12 is essential for migration of activated Langerhans cells from epidermis to dermis. *Eur J Immunol.* 2008; 38:3050–3059. [PubMed: 18924211]
55. Okada T V, Ngo N, Ekland EH, Forster R, Lipp M, Littman DR, Cyster JG. Chemokine requirements for B cell entry to lymph nodes and Peyer’s patches. *J Exp Med.* 2002; 196:65–75. [PubMed: 12093871]
56. Blades MC, Ingegnoli F, Wheller SK, Manzo A, Wahid S, Panayi GS, Perretti M, Pitzalis C. Stromal cell-derived factor 1 (CXCL12) induces monocyte migration into human synovium transplanted onto SCID Mice. *Arthritis Rheum.* 2002; 46:824–836. [PubMed: 11920421]
57. Blades MC, Manzo A, Ingegnoli F, Taylor PR, Panayi GS, Irjala H, Jalkanen S, Haskard DO, Perretti M, Pitzalis C. Stromal cell-derived factor 1 (CXCL12) induces human cell migration into human lymph nodes transplanted into SCID mice. *J Immunol.* 2002; 168:4308–4317. [PubMed: 11970972]
58. Bachmann MF, Kopf M, Marsland BJ. Chemokines: more than just road signs. *Nat Rev Immunol.* 2006; 6:159–164. [PubMed: 16491140]
59. Stutte S, Quast T, Gerbitzki N, Savinko T, Novak N, Reifemberger J, Homey B, Kolanus W, Alenius H, Forster I. Requirement of CCL17 for CCR7- and CXCR4-dependent migration of cutaneous dendritic cells. *Proc Natl Acad Sci U S A.* 107:8736–8741. [PubMed: 20421491]
60. Kabashima K, Shiraishi N, Sugita K, Mori T, Onoue A, Kobayashi M, Sakabe J, Yoshiki R, Tamamura H, Fujii N, Inaba K, Tokura Y. CXCL12-CXCR4 engagement is required for migration of cutaneous dendritic cells. *Am J Pathol.* 2007; 171:1249–1257. [PubMed: 17823289]
61. Vanbervliet B, Bendriss-Vermare N, Massacrier C, Homey B, de Bouteiller O, Briere F, Trinchieri G, Caux C. The inducible CXCR3 ligands control plasmacytoid dendritic cell responsiveness to the constitutive chemokine stromal cell-derived factor 1 (SDF-1)/CXCL12. *J Exp Med.* 2003; 198:823–830. [PubMed: 12953097]

62. Kabashima K, Sugita K, Shiraishi N, Tamamura H, Fujii N, Tokura Y. CXCR4 engagement promotes dendritic cell survival and maturation. *Biochem Biophys Res Commun.* 2007; 361:1012–1016. [PubMed: 17679142]
63. Howe AK. Regulation of actin-based cell migration by cAMP/PKA. *Biochim Biophys Acta.* 2004; 1692:159–174. [PubMed: 15246685]
64. Howe AK, Baldor LC, Hogan BP. Spatial regulation of the cAMP-dependent protein kinase during chemotactic cell migration. *Proc Natl Acad Sci U S A.* 2005; 102:14320–14325. [PubMed: 16176981]
65. Friedl P, Weigelin B. Interstitial leukocyte migration and immune function. *Nat Immunol.* 2008; 9:960–969. [PubMed: 18711433]
66. Wei SH, Parker I, Miller MJ, Cahalan MD. A stochastic view of lymphocyte motility and trafficking within the lymph node. *Immunol Rev.* 2003; 195:136–159. [PubMed: 12969316]
67. Miller MJ, Hejazi AS, Wei SH, Cahalan MD, Parker I. T cell repertoire scanning is promoted by dynamic dendritic cell behavior and random T cell motility in the lymph node. *Proc Natl Acad Sci U S A.* 2004; 101:998–1003. [PubMed: 14722354]
68. Bagley KC, Abdelwahab SF, Tuskan RG, Fouts TR, Lewis GK. Cholera toxin and heat-labile enterotoxin activate human monocyte-derived dendritic cells and dominantly inhibit cytokine production through a cyclic AMP-dependent pathway. *Infect Immun.* 2002; 70:5533–5539. [PubMed: 12228279]
69. Bagley KC, Abdelwahab SF, Tuskan RG, Fouts TR, Lewis GK. Pertussis toxin and the adenylate cyclase toxin from *Bordetella pertussis* activate human monocyte-derived dendritic cells and dominantly inhibit cytokine production through a cAMP-dependent pathway. *J Leukoc Biol.* 2002; 72:962–969. [PubMed: 12429718]
70. Anosova NG, Chabot S, Shreedhar V, Borawski JA, Dickinson BL, Neutra MR. Cholera toxin, *E. coli* heat-labile toxin, and non-toxic derivatives induce dendritic cell migration into the follicle-associated epithelium of Peyer's patches. *Mucosal Immunol.* 2008; 1:59–67. [PubMed: 19079161]
71. Dertzbaugh, MT.; Elson, CO. Cholera toxin as a mucosal adjuvant. In: Spriggs, DR.; Koff, WC., editors. *Topics in vaccine adjuvant research.* CRC Press; Boca Raton: 1990. p. 119-131.
72. Freytag LC, Clements JD. Bacterial toxins as mucosal adjuvants. *Curr Top Microbiol Immunol.* 1999; 236:215–236. [PubMed: 9893362]
73. Lycke N, Holmgren J. Strong adjuvant properties of cholera toxin on gut mucosal immune responses to orally presented antigens. *Immunology.* 1986; 59:301–308. [PubMed: 3021614]
74. Dickinson BL, Clements JD. Dissociation of *Escherichia coli* heat-labile enterotoxin adjuvanticity from ADP-ribosyltransferase activity. *Infect Immun.* 1995; 63:1617–1623. [PubMed: 7729864]
75. Yarwood SJ, Borland G, Sands WA, Palmer TM. Identification of CCAAT/enhancer-binding proteins as exchange protein activated by cAMP-activated transcription factors that mediate the induction of the SOCS-3 gene. *J Biol Chem.* 2008; 283:6843–6853. [PubMed: 18195020]
76. Borland G, Bird RJ, Palmer TM, Yarwood SJ. Activation of protein kinase C alpha by EPAC1 is required for the ERK- and C/EBPbeta-dependent induction of the SOCS-3 gene by cyclic AMP in COS1 cells. *J Biol Chem.* 2009
77. Mazzoni A, Segal DM. Controlling the Toll road to dendritic cell polarization. *J Leukoc Biol.* 2004; 75:721–730. [PubMed: 14726500]
78. Xiao BG, Huang YM, Link H. Dendritic cell vaccine design: strategies for eliciting peripheral tolerance as therapy of autoimmune diseases. *BioDrugs.* 2003; 17:103–111. [PubMed: 12641489]

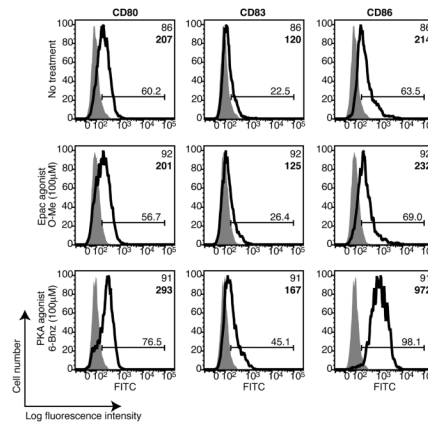


Figure 1.

Selective activation of PKA, but not Epac, increases dendritic cell expression of co-stimulatory molecules. Immature DCs were treated with 6-Bnz-cAMP (100µM) or O-Me-cAMP (100µM) for 24 h and the surface expression of CD80, CD83 and CD86 was determined by flow cytometry. Grey histograms indicate the isotype controls and the markers are depicted as bold line histograms. The MFIs are indicated in the upper right hand corners of the histograms in standard type for the isotype controls and bold type for the markers. Data are representative of two independent experiments.

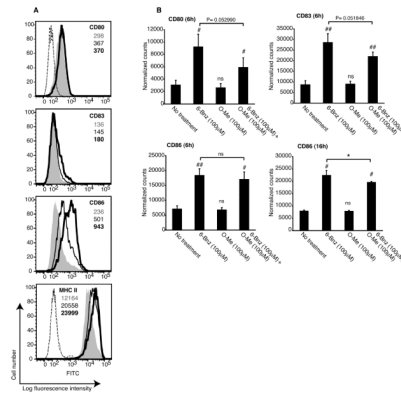


Figure 2.

Epac signaling antagonizes the effect of PKA on dendritic cell expression of co-stimulatory molecules and MHC class II. *A*, Immature DCs were treated with 6-Bnz-cAMP (100 μ M; bold line histograms) or a combination of 6-Bnz-cAMP and O-Me-cAMP (both 100 μ M; thin line histograms) for 24 h and the surface expression of CD80, CD83, CD86 and MHC class II was determined by flow cytometry. Grey histograms represent staining of non-treated immature DCs. MFIs for CD80, CD83, CD86 and MHC class II are indicated in grey type for non-treated immature DCs, bold type for 6-Bnz-cAMP-treated DCs, and standard type for DCs treated with both 6-Bnz-cAMP and O-Me-cAMP. The MFI of the IgG1 isotype controls for CD80, CD83 and CD86 are as follows: 101 for non-treated DCs (dotted line), 98.5 for 6-Bnz-cAMP treated DCs (long dashed line) and 102 for DCs treated with both agonists (dashed line). The MFI of the IgG2a isotype controls for MHC class II are as follows: 140 for non-treated DCs (dotted line), 140 for 6-Bnz-cAMP treated DCs (long dashed line) and for 137 DCs treated with both agonists (dashed line). Data are representative of two independent experiments. *B*, Immature DCs were treated with 6-Bnz-cAMP (100 μ M), O-Me-cAMP (100 μ M) or a combination of 6-Bnz-cAMP and O-Me-cAMP (both 100 μ M) for 6 or 16 h after which RNA was extracted and transcripts encoding CD80, CD83 and CD86 were quantified by digital mRNA profiling. The results are expressed as the mean \pm SEM of duplicate measurements from three independent experiments for the 6 h data and two independent experiments for the 16 h data.

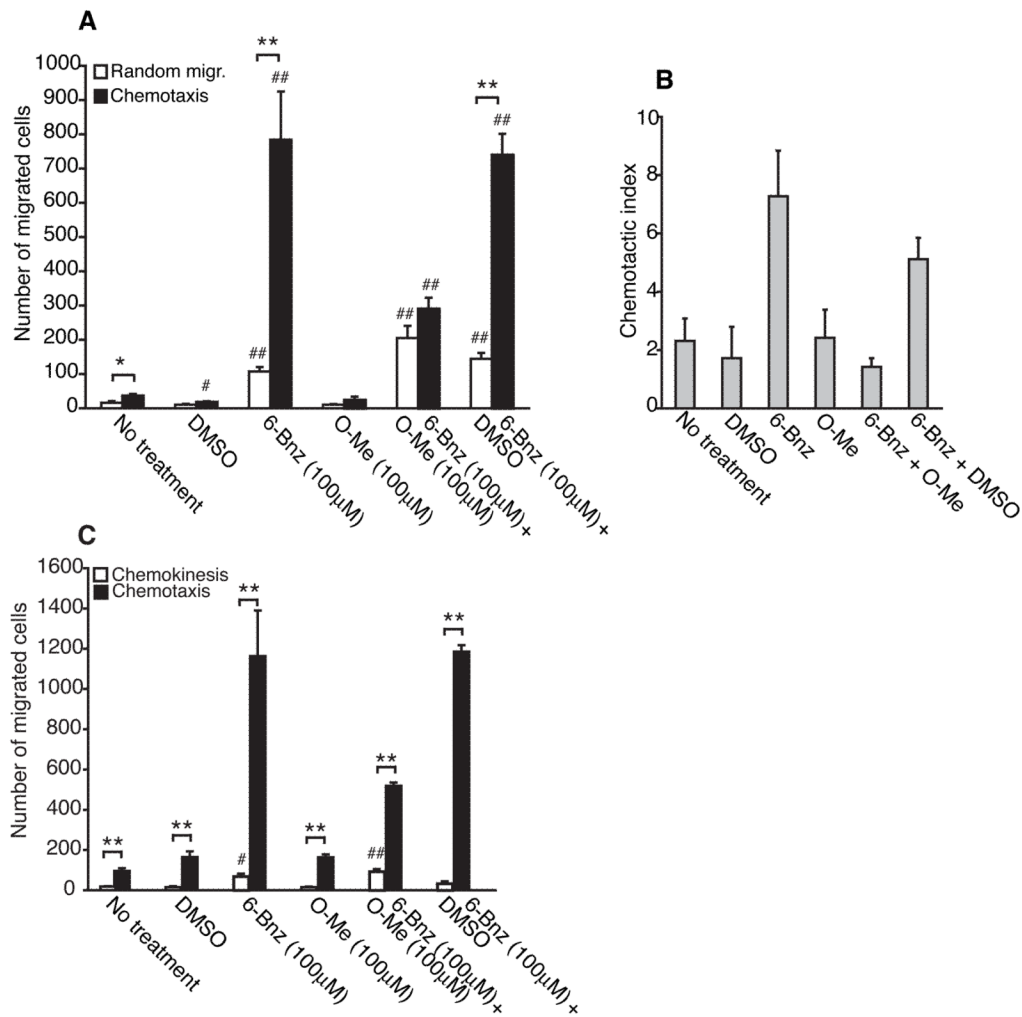


Figure 3.

Crosstalk between the PKA and Epac signaling pathways regulates DC chemotaxis to CXCL12. *A* and *B*, Immature DCs were treated with DMSO (0.25%), 6-Bnz-cAMP (100μM), O-Me-cAMP (100μM), a combination of 6-Bnz-cAMP and O-Me-cAMP (both 100μM) or a combination of 6-Bnz-cAMP (100μM) and DMSO (0.25%) for 24 h and examined for random migration and chemotaxis to CXCL12 (100ng/ml). Means ± SEM of triplicate measurements from one of three independent experiments are shown in panel *A* and the chemotactic index is displayed in panel *B*. *C*, Immature DCs were treated as described above and examined for chemotaxis to CXCL12, random migration and chemokinesis. Means ± SEM of triplicate measurements from one of three independent experiments is shown.

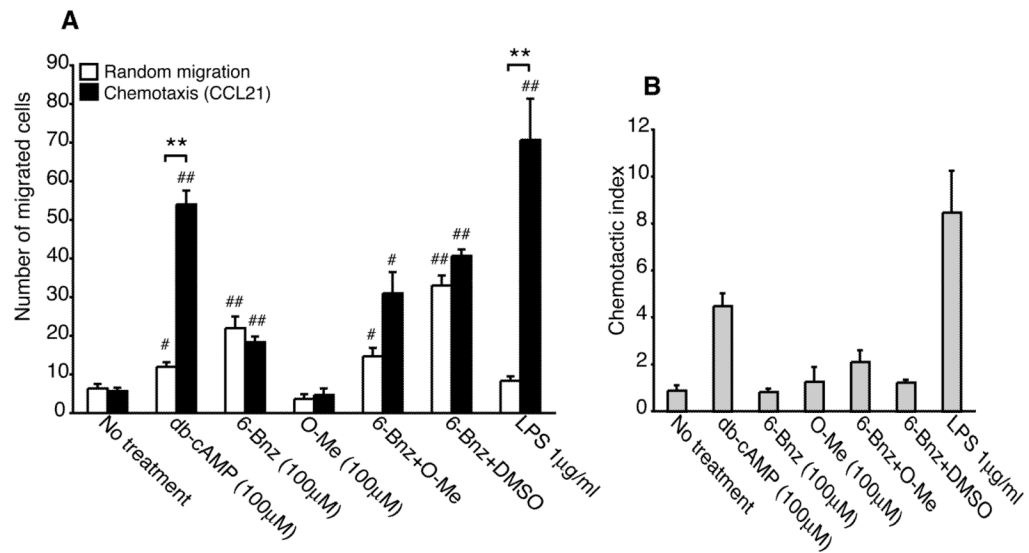


Figure 4.

PKA-Epac crosstalk does not regulate DC chemotaxis to CCL21. *A* and *B*, Immature DCs were treated with db-cAMP (100μM), 6-Bnz-cAMP (100μM), O-Me-cAMP (100μM), a combination of 6-Bnz-cAMP and O-Me-cAMP (both 100μM), a combination of 6-Bnz-cAMP (100μM) and DMSO (0.25%) or LPS (1μg/ml) for 24 h and examined for random migration and chemotaxis to CCL21 (100ng/ml). Means ± SEM of triplicate measurements from one of three independent experiments are shown in panel *A* and the chemotactic index is displayed in panel *B*.

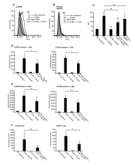


Figure 5.

PKA-Epac crosstalk regulates dendritic cell expression of CXCR4. *A* and *B*, Immature DCs were treated with 6-Bnz-cAMP (100 μ M), O-Me-cAMP (100 μ M) or a combination of 6-Bnz-cAMP and O-Me-cAMP (both 100 μ M) for 24 h and CXCR4 expression was quantified by flow cytometry. Staining for CXCR4 is shown in panel *A* and the IgG2a isotype control antibody is shown in *B*. Data are representative of three independent experiments. *C*, Immature DCs were treated with 6-Bnz-cAMP (100 μ M), O-Me-cAMP (100 μ M), a combination of 6-Bnz-cAMP and O-Me-cAMP (both 100 μ M) or a combination of 6-Bnz-cAMP (100 μ M) and DMSO (0.25%) for 24 h and CXCR4 expression was quantified by flow cytometry. The MFI (means \pm SEM) from three independent experiments is shown. *D–F*, Immature DCs were treated with 6-Bnz-cAMP (100 μ M), O-Me-cAMP (100 μ M) or a combination of 6-Bnz-cAMP and O-Me-cAMP (both 100 μ M) for 6 and 16 h after which RNA was extracted and transcripts encoding CXCR4 isoform 1 (*D*) and isoform 2 (*E*) and CXCR7 (*F*) were quantified by digital mRNA profiling. The results are expressed as the mean \pm SEM of duplicate measurements from three independent experiments for the 6 h data and two independent experiments for the 16 h data.

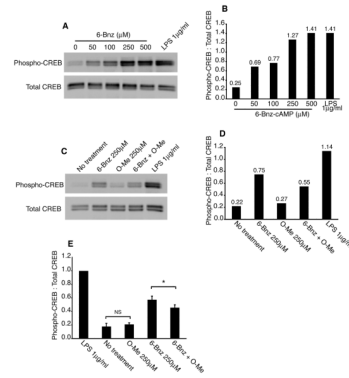


Figure 6.

Epac reduces PKA phosphorylation of CREB. *A* and *B*, Immature DCs were treated with 6-Bnz-cAMP (50–500 μ M) for 30 min at 37°C after which phospho-CREB and total CREB were detected in lysates by immunoblot (*A*). Band intensities were determined by densitometry and the phospho-CREB signal was normalized to total CREB (*B*). Data from one representative experiment is shown. *C* and *D*, Immature DCs were treated with 6-Bnz-cAMP (250 μ M), O-Me-cAMP (250 μ M), a combination of 6-Bnz-cAMP and O-Me-cAMP (both 250 μ M) or LPS (1 μ g/ml) for 30 min at 37°C. Cells were then lysed and phospho-CREB and total CREB were detected in lysate by immunoblot (*C*). Band intensities were determined by densitometry and the phospho-CREB signal was normalized to total CREB (*D*). One representative experiment of four independent experiments is shown. *E*, Immature DCs were treated as described in (*C*). Data are from four independent experiments in which the phospho-CREB-to-total CREB signals were normalized to that of the LPS-treated DCs (= 1.0).

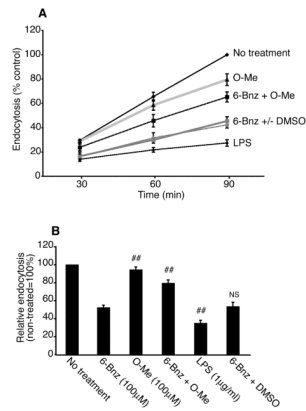


Figure 7.

Crosstalk between PKA and Epac regulates dendritic cell endocytosis. *A* and *B*, Immature DCs were treated with 6-Bnz-cAMP (100µM), O-Me-cAMP (100µM), LPS (1µg/ml), a combination of 6-Bnz-cAMP and O-Me-cAMP (both 100µM) or a combination of 6-Bnz-cAMP (100µM) and DMSO (0.25%) for 24 h. Then, cells were incubated with FITC-dextran (1mg/ml) for 30, 60 and 90 min at 4°C or 37°C. FITC-dextran uptake was measured by flow cytometry. In each experiment, the MFI of the 4°C controls was subtracted from the MFI of the 37°C samples. *A*, MFIs for treated DCs were normalized to the MFI of non-treated DCs incubated with FITC-dextran for 90 min (= 100%). Means ± SEM of single measurements for each time point from three independent experiments are shown. *B*, MFIs for treated DCs were normalized to the MFI of non-treated DCs at each time point. The results are expressed as the mean ± SEM of all three time points (30, 60 and 90 min) from three independent experiments. Statistical significance between PKA agonist-treated DCs and DCs treated with the Epac agonist, the PKA and Epac agonists in combination, LPS or the PKA agonist in combination with DMSO is denoted by * (p<0.05) and ## (p<0.01); NS = not statistically significant.

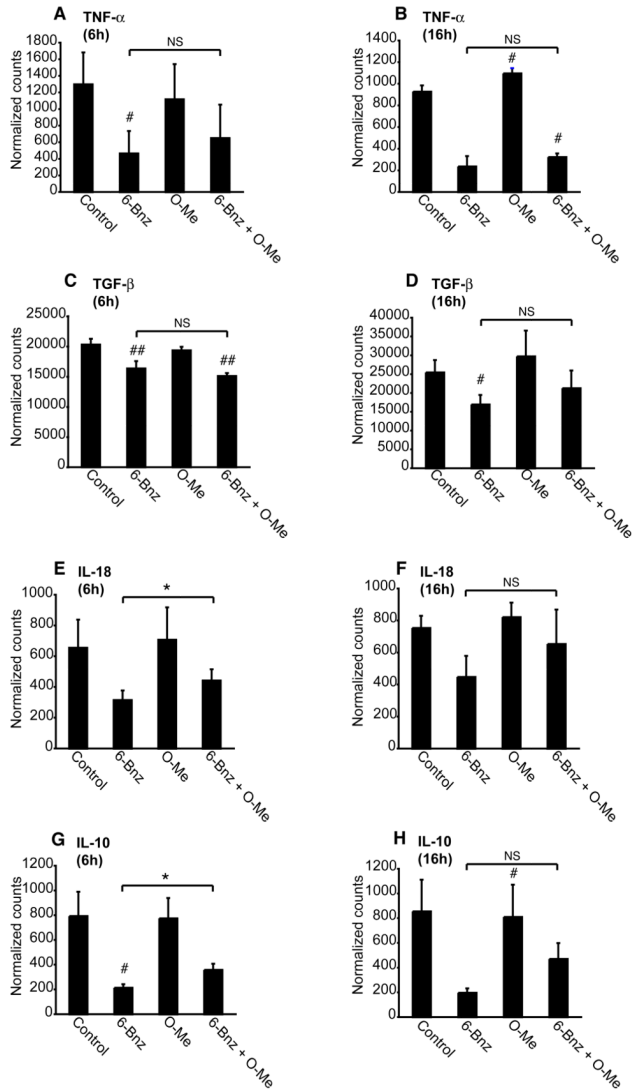


Figure 8. PKA-Epac crosstalk regulates dendritic cell cytokine expression. *A-H*, Immature DCs were treated with 6-Bnz-cAMP (100 μ M), O-Me-cAMP (100 μ M) or a combination of 6-Bnz-cAMP and O-Me-cAMP (both 100 μ M) for 6 and 16 h after which RNA was extracted and transcripts encoding TNF- α , TGF- β , IL-18 and IL-10 were quantified by digital mRNA profiling. The results are expressed as the mean \pm SEM of duplicate measurements from three independent experiments for the 6 h data and two independent experiments for the 16 h data.

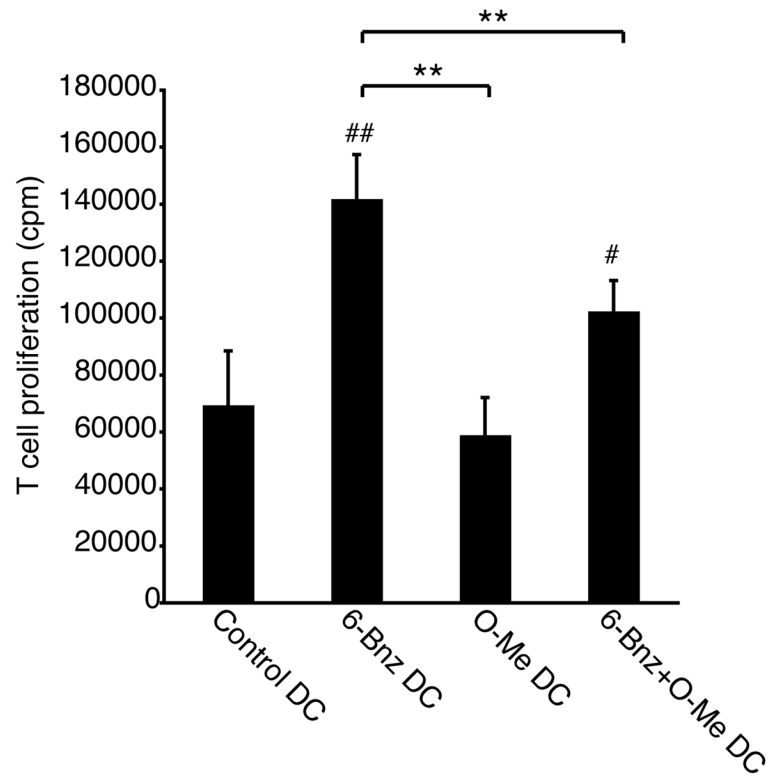


Figure 9.

PKA-Epac crosstalk regulates dendritic cell activation of T cells. Immature DCs were treated with 6-Bnz-cAMP (100 μ M), O-Me-cAMP (100 μ M) or a combination of 6-Bnz-cAMP and O-Me-cAMP (both 100 μ M) for 24 h after which cells were washed and incubated with allogeneic T cells for 5 days. During the last 18 h of incubation, cultures were spiked with 1 μ Ci 3 H-methyl-thymidine and thymidine incorporation into proliferating T cells was quantified by scintillation counting. The results are expressed as the mean \pm SEM of triplicate measurements from two independent experiments performed with cells from different donors.